

Sparse OBN acquisition in shallow water at CCS Sleipner field: the role of multiples in FWI

Sandrine David*, Eddie Cho, Graeme Stock, Fons ten Kroode, M.A.H Zuberi, TGS

Summary

Acquiring surface seismic data over carbon storage sites can be challenging, particularly in shallow water environments where co-located structures such as platforms, production facilities and windfarms are and will be more prevalent. Moreover, CCS monitoring solutions need to be more cost effective than monitoring of Oil and Gas reservoirs. In response to these challenges, innovative acquisition solutions were tested at the Sleipner field, where Equinor has been sequestering CO₂ since 1996.

A short streamer acquisition (XHR) was acquired to obtain a high-resolution image of the subsurface. In parallel, Ocean Bottom Nodes (OBN) were deployed on a sparse grid in order to derive a velocity model using Full Waveform Inversion (FWI). Sparse node acquisition has limitations, notably in the sampling of the very shallow subsurface and this can compromise high frequency velocity updates. To ameliorate this issue, our work leverages multiples to stabilize and enhance the accuracy of the velocity models obtained with FWI, which then enables robust and reliable monitoring of CCS sites.

Introduction

Ocean bottom nodes were deployed in the Sleipner area over the CCS injection site to complement the high-resolution short streamers acquisition, with the aim to derive a velocity model using FWI for imaging of the XHR data. Employing a cost-effective approach, free-falling nodes were released and equipped with a “pop-up” recovery mechanism to enable equally optimized recovery. To optimize the cost further, we have used a limited number of nodes on a sparse grid (500 x 525 m). Our objective was to evaluate FWI capabilities in CCS shallow water context (80m here).

Achieving a high-resolution velocity model with FWI necessitates adequate illumination and data coverage. At low frequencies, FWI predominantly relies on diving wave energy where the sparsity of the nodes is not a problem whereas higher frequencies updates rely more heavily on reflection energy.

Despite recording node data simultaneously with XHR data using shots fired from the streamer vessel, which generated a dense shot carpet (6.25m x 75m), the OBN only FWI image lacked illumination due to the sparse nodal grid. To enhance the shallow coverage, both spatially and temporally, we leverage the advantages of multiples containing near-angle information, rather than relying solely on primary

reflection data. Our study demonstrates that multiples add value to the FWI results.

We conducted various tests to demonstrate this, including the following comparisons:

- 25Hz FWI results derived using both pre-processed data (Up/Down Deconvolution (UDD) data (i.e multiples removed)) and a limited processing dataset more akin to a raw hydrophone (full wavefield).
- 60Hz FWI Image (derivative of the FWI velocity model) against the processed and raw XHR stack data.
- 8Hz FWI results derived using both a raw hydrophone data (full wavefield) and a “primaries only” hydrophone data modeled in the 60 Hz FWI model.

Up/Down Deconvolution (UDD) versus “raw” Hydrophone results

As a first step, Dynamic Matching FWI (DM FWI) (Mao et al. 2020) was run up to 8 Hz, using diving wave and near surface reflection energy. Subsequently, higher frequency updates were performed up to 25Hz where two approaches were explored.

1. Both hydrophone and vertical geophone components were processed through to UDD, providing a dataset with the surface reflection events (ghosts and surface multiples) removed.
2. Full wavefield hydrophone (P) dataset which included free surface reflectivity which was subsequently used in the inversion. As the data had minimum pre-processing applied (de-bubble only), a data reconstruction FWI (Zuberi et al., 2023) was employed to mitigate elastic effects.

Both types of datasets were used separately as an input to the FWI process, up to 25Hz. In the first case, FWI was run without the reflective free surface whereas it was needed for the second scenario. At a later stage, FWI was run up to 60Hz using the hydrophone data only.

Figure 1 shows the velocity models after the 25 Hz update from the two methods, along with FWI images derived from these models. Notably, the CO₂ plume manifests itself as a distinct slow velocity area. While both updates delineate the CO₂ plume well, the UDD dataset has less definition in the shallow part of the velocity model due to the limited illumination provided by the sparse nodal grid, which is especially evident in the FWI images (green arrows). Additionally, the UDD version exhibits fast velocity bands (red arrows), absent in the full wavefield results.

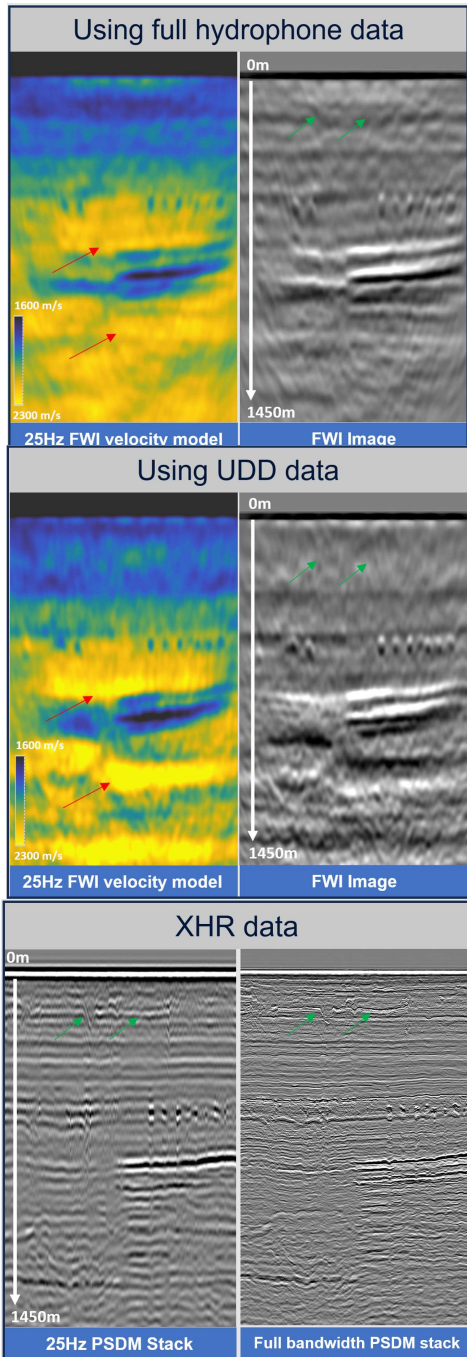


Figure 1: Comparisons of the velocity models and FWI images for the 25 Hz updates produced using UDD reflectivity data vs the full wavefield (P) data. XHR stack data is also shown for reference.

Further evaluation was conducted comparing the flatness of common image gathers (CIGs) of the UDD data, after Kirchhoff depth migration using the two different velocity models. Figure 2 compares CIGs for both cases. The red arrows marked on the gathers indicate key events around the CO₂ plume where gather flatness is significantly improved in the full wavefield result compared to the UDD, correlating with the presence of fast velocity bands in the UDD reflectivity velocity model.

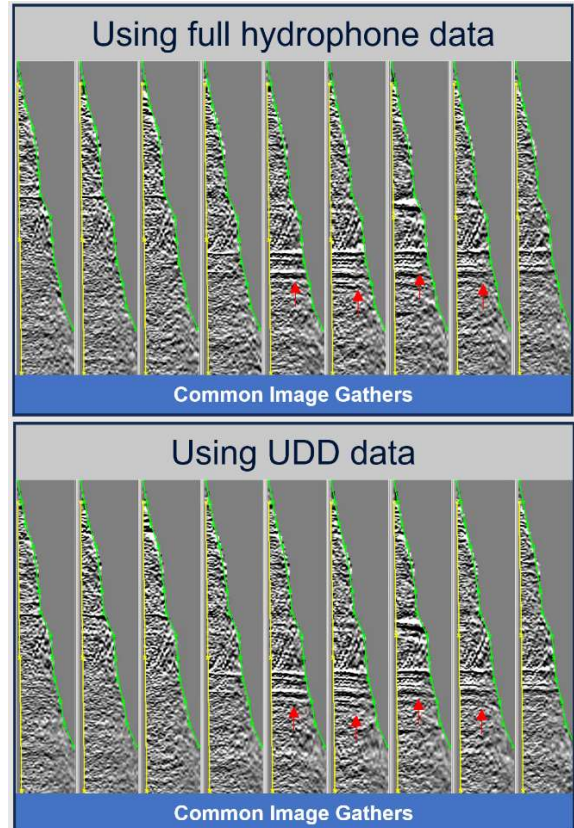


Figure 2: Comparisons of common image gathers, migrated UDD data with the 25 Hz velocity model update produced using UDD reflectivity data vs the full wavefield (P) data.

60Hz FWI image compared to acquired seismic data

The initial phase of the work was to derive a velocity model for imaging the XHR data. The 25Hz velocity model update using the full wavefield hydrophone data provided the necessary update to achieve this intent. In a second step, we wanted to push the limits of FWI on this sparse node deployment and obtained a high-resolution velocity model update and FWI image.

With the ambition of being able to distinguish the thin sand layers in which the CO₂ migrated, a high resolution velocity

model was generated using a FWI workflow with a maximum frequency of a 60 Hz. For this workflow, the full wavefield hydrophone data was used, FWI updates were run by incrementing frequency bands input at each pass up to 60Hz.

The 60 Hz velocity update and its corresponding FWI image were subsequently compared to a migrated UDD section. To further validate the model, comparisons were made with depth migrated XHR data, both fully processed and raw (including multiples). The comparisons, detailed in Figure 3, show that the 60Hz FWI image aligns well with both the UDD and XHR migrated sections. Notably, the presence of multiples in the raw XHR image is absent in the FWI image, indicating the reliability of utilizing the full wavefield for updates at higher frequencies. Red boxes indicate injectites multiples which are clearly neither present on the UDD image nor on the FWI image.

Worth noting that although the resolution at the CO₂ plume was satisfactory – as we could interpret nine sand layers – the overall resolution, especially at the shallow area, was not as high as we would have expected based in the frequency content from the input data.

FWI without free surface performed on primaries only data

An additional test was run to further assess the impact of free surface multiples in a sparse node and shallow water configuration. A ‘primaries only’ dataset was generated, using the 60Hz velocity model, through acoustic finite difference modelling with an absorbing free surface condition. The synthetic data was subsequently used in an FWI sequence (up to 8Hz), again with an absorbing free surface condition in the forward modelling. Figure 4 shows the velocity updates at 8 Hz for both the full wavefield and the synthetic primaries only data. The resulting velocity model from the primaries only data exhibits anomalously high velocity regions in the shallow section where imprint of the sparse node sampling is evident. Additionally, high velocities are also observed above the plume resulting in poor gather flatness in common image gathers (red arrows) and poor imaging and erroneous imaged reflection events in the migrated stack. This highlights the benefit of using the full wavefield as it provides enhanced illumination of the shallow subsurface through multiple energy, which cannot be achieved using primaries only.

Conclusion and way forward

Our study highlights the feasibility of addressing sparse OBN grid acquisition in shallow water environment through the exploitation of multiples in the FWI process. By leveraging multiples, we successfully achieved a high-resolution velocity model update using only a small set of nodes.

Additional tests will be performed to increase our understanding of FWI work in shallow water. A multi-client OBN survey has recently been acquired in the Sleipner area, covering the CCS part as well, with a dense OBN grid (50m x 300m). Decimation tests will be performed to assess the impact of the node and shot density in the FWI results.

Furthermore, additional developments in the inversion process will be done in order to increase the resolution and ensure better and more reliable velocity model updates in the shallow areas.

These test results will unlock the potential to integrate OBN data in CCS projects, offering enhanced efficiency and accuracy in subsurface imaging and characterization.

Acknowledgments

The authors thank Equinor Energy ASA and CLIMIT program for their support and collaboration on the XHR/OBN Sleipner acquisition.

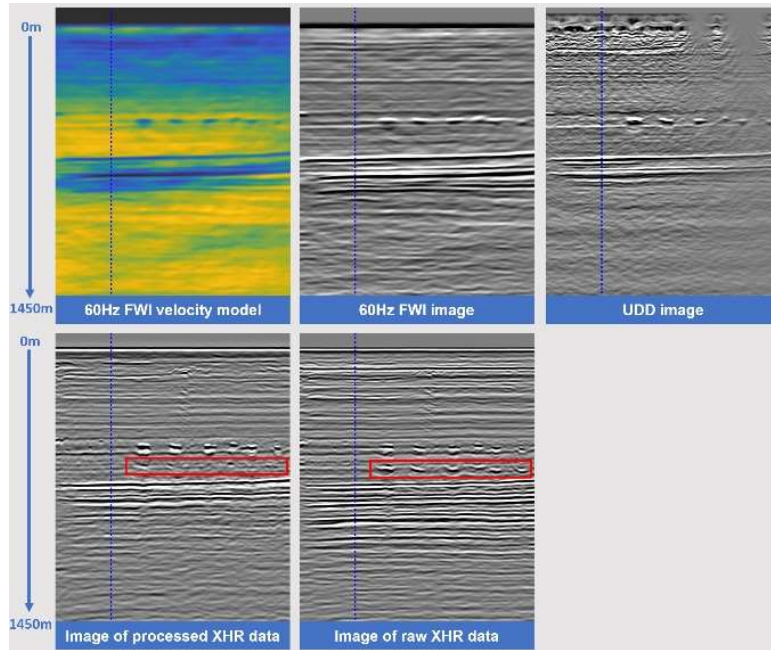


Figure 3: Comparison of 60 Hz FWI velocity model with derived image, migrated UDD dataset, migrated XHR (processed) dataset and migrated XHR (Raw) dataset. Red boxes show area with evident injectites multiples in the XHR data but not observed in the OBN data or FWI results.

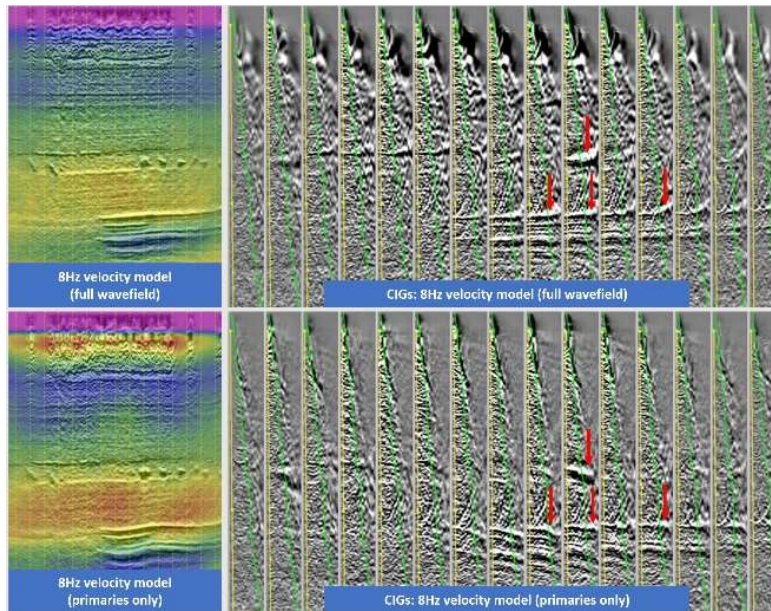


Figure 4: 8 Hz velocity model overlays on KPSDM imaged UDD data and common image gathers comparing results using the full wavefield input vs primaries only data. Red arrows show example area where gather flatness is better on the full wavefield (P) results.